Simulating the effects of a virtual motorcycle passenger on vehicle motion and rider effort

Samuel L. Milhaven[1], *Member, IEEE*, Wenjia Li[2], Robert McClosky[2], and Alexander A. Brown[3], *Member, IEEE*

***Abstract*—Motorcycles, bicycles, and other single-track vehicles are popular but dangerous methods of transportation. While some are piloted by only a single rider, many powered two-wheelers are ridden with a passenger, who may also significantly influence the vehicle's dynamics. Because simulations are a critical component of vehicle safety research, this paper asks whether a simulated, active "virtual passenger" has stabilizing or destabilizing effects on a rider-vehicle-passenger system. This virtual passenger exerts its control effort by moving an inverted pendulum to simulate the motion of a human passenger's torso without explicit knowledge of rider inputs. A battery of simulations in the nonlinear, multi-body Webots robot simulator show that the passenger's control efforts have mixed effects on both rider effort and vehicle stability over abrupt transitions in pavement height. This indicates that the inclusion of passenger motion may be critical when vetting the safety of roadway designs and/or emerging motorcycle technologies like Advanced Rider Assist Systems.**

***Index Terms*—Safety Verification and Validation Techniques; Vulnerable Road User Protection Strategies; Real-World Testing Methodologies for Safety Systems; motorcycle safety; powered two-wheeler; single-track vehicles**

I. Introduction

Motorcycles are a popular and common mode of transportation all over the world due to their compact size and affordability. However, they are also quite dangerous, with a significant risk of rider injury or death during operation. According to the National Safety Council, "Although motorcycles make up only 3% of all registered vehicles and 0.6% of all vehicle miles traveled in the United States, motorcyclists accounted for 14% of all traffic fatalities, 17% of all occupant fatalities, and 3% of all occupant injuries in 2021" [1]. While much of this risk comes from motorcycles' interaction with other traffic, some is because motorcycles are only open-loop stable at certain forward velocities. Outside of their self-stable speed range, they require frequent control inputs from the rider for stabilization. Even with a skilled rider, driving over uneven road surfaces, such as curbs, broken edges, and rutted pavement can excite dynamics that are difficult to control and may lead to crashes. In addition, many motorcycles carry passengers, and [2] and [3] found that passenger motion can have a significant effect on rider steering torque. But it's possible that experienced passengers may also *improve* a motorcycle's stability by active balancing, and their additional control authority may actually help motorcycles and their riders navigate disturbances, such as those common during transitions across uneven pavement. While dynamic testing of motorcycles poses a significant risk to human riders, self-driving motorcycles and/or simulations offer safer alternatives for testing as part of the development and validation of advanced rider assist systems, policies related to road geometry or other infrastructure, and even as surrogates for evaluating the detection of motorcycles by self-driving cars and trucks. Because motorcycle passengers may have either adverse or helpful effects on human-ridden motorcycle dynamics, evaluating how an artificial, virtual "passenger" might change the closed-loop dynamics of a self-driving motorcycle could help build better test vehicles for all of the use cases summarized above.

In [4], Li et al. developed the "Webikes" vehicle simulation element for the Webots robot simulator [5], and found that Webots has promise as an open-source platform for motorcycle safety simulations. However, that study's control system for the motorcycle only included a virtual rider, and had no provisions for studying passenger behavior. Building on that study to improve the capability of the "Webikes" simulation element, and to answer questions about how passenger motion can affect overall vehicle stability and performance, the present study explores the development of an "active passenger" that researchers can use when simulating motorcycles in Webots.

Mimicking the way a human passenger can influence a motorcycle's dynamics, our virtual passenger has partial, inferred knowledge of the motorcycle's closed-loop roll dynamics but can only influence its motion through torso lean. Like a human passenger, it has no knowledge of rider inputs or the motion of the motorcycle's steered, front frame. In the following sections, we explore whether such a virtual passenger will improve or erode a self-driving motorcycle's stability and/or disturbance rejection capability as it traverses an uneven pavement edge, such as those common in road construction zones.

The remainder of this paper is organized as follows. Section II reviews related work, and Section III outlines the closed loop rider-vehicle model and the model for the active passenger. Section IV outlines the design of the Linear Quadratic Regulator (LQR) controller used to control the balancer in simulation. Section V outlines the design of

[1]Departments of Electrical Engineering and Computer Engineering and Mechanical and Industrial Engineering, Northeastern University, Boston, Massachusetts, United States; milhaven.s@northeastern.edu

[2]Integrative Engineering Program, Lafayette College, Easton, Pennsylvania, United States

[3]Department of Mechanical Engineering, Lafayette College, Easton, Pennsylvania, United States; brownaa@lafayette.edu

a battery of simulations in the Webots multi-body robot simulation software [5] to test the passenger balance model when subjected to a spread of road geometry configurations similar to those studies in [4]. Sections VI and VII discuss the results of the simulations conducted, along with limitations and next steps for future work.

II. Related Work

A. Dynamic Models of Motorcycle and Rider Behavior

In the interest of understanding two-wheeled vehicle stability and control, canonical linear models have emerged, such as those in [6], [7] that capture their dynamics in varying levels of detail. One of the oldest and most influential models is the Whipple Model [6], a 4th-order, linear model of bicycle dynamics. Since the development of the Whipple Model, similar models that consider driver steer angle [8], [9] and/or driver torque at the handlebars [7]–[10] have become common. Some maintain the Whipple model's no-slip tire assumption [11], and others use a tire model allowing a linear [12] or non-linear [13] relationship between tire slip and tire force. Many research groups have determined either experimentally, analytically, or through simulation that autonomous motorcycles can be actively stabilized using actuation about the steering axis only [14]–[20].

In an attempt to represent rider inputs from both rider torso motion and steering action, some researchers have simulated virtual riders that use torque about both the steering axis and the roll axis for stabilization [7]–[9], [21], [22], even building and testing robotic two-wheeler prototypes [10], [23], [24] that use a combination of steer control and lean torque to stabilize. The literature indicates that including the rider-lean-torque as a system input improves a vehicle's ability to stabilize at various speeds [10]. Additionally, rider lean torque alone can allow a single-track vehicle to stabilize itself at low speeds and even while completely stationary [10], [23]. Therefore, including a mechanical approximation of rider torque in addition to steering torque as inputs allows an autonomous single-track vehicle to stabilize at all speeds and perform complex maneuvers. In modeling the lean torque of a motorcycle rider, there is a bifurcation in how "rider torque" is represented, with some researchers using flywheels [23]–[25] and others using an inverted pendulum [10].

In studies where both lean and steer action are used to model a human rider, such as in [10] and [11], the motorcycle controller uses all states of the combined vehicle/driver system. However, real motorcycles may be subject to control inputs from a passenger's body motion as well as the rider's body motion.

B. Motorcycle Passengers

Passengers on real, human-driven motorcycles are unique in that they are not directly aware of the rider inputs that stabilize the vehicle. The information they do have access to is limited to vehicle rear frame motion (e.g., roll and roll rate), along with measurements of their own ego motion relative to the rear frame. In [2] and [3], Koizumi et al. found that in certain instances while traveling on smooth, flat ground, disturbance inputs from a passenger's lean required increased driver steer torque input to stabilize the system. However, passengers have an interest in maintaining vehicle stability, which means that they may also be attempting to correct unexpected vehicle motion by using their torso. While [2] and [3] investigated how passenger motion might require *more* corrective action by a motorcycle pilot, it is unclear from the literature whether a passenger whose "goal" is to improve vehicle disturbance rejection might actually improve the total vehicle-rider-passenger system's performance when encountering an unexpected road feature such as a change in pavement height. Prior work on motorcycle passengers is scarce, and to the authors' knowledge, no prior study has been conducted that investigates the development of a virtual passenger with the limitations described here (in regards to limited vehicle state feedback and limited knowledge of the rider's actions).

Our work intends to address this current gap in research by developing a virtual passenger that can simulate the behavior of a human passenger with limited knowledge of the motorcycle system in a realistic manner.

III. Vehicle-Rider-Passenger Model

A. Vehicle-Rider Model

Our approach was to allow our virtual active passenger (in contrast to a rigidly attached, nonmoving passenger) to "ride" a motorcycle that is already equipped with a separate virtual rider. The virtual rider is responsible for primary vehicle stabilization using steering action, and the virtual active passenger is responsible for relatively naïve additional stabilization and disturbance rejection efforts using torso lean alone. This is in contrast to studies such as [10], where a rider with knowledge of all vehicle states combines lean and steering. Our virtual rider is based on the standard "Webikes" rider outlined in [4]. It was designed using a Whipple Bicycle Model [6] for the vehicle, which we used to synthesize an LQR with steering input at $11.2m/s$. The LQR design assumed that the total vehicle mass and mass center location were inclusive of both the rider and a "rigidly attached" passenger, representing an implicit assumption that the rider would move with the rear frame of the motorcycle. The dynamics of the closed loop vehicle-rider-rigid passenger system are shown in Fig. 1, along with a fit for a second-order transfer function in standard form that represents the passenger's "internal model" of the closed loop vehicle-rider system. Based on that transfer function, the virtual passenger conceptualizes the closed-loop vehicle-rider system as a torsional spring-mass-damper in the synthesis of its own controller design. This is intended to represent the fact that a human passenger can learn how the motorcycle behaves under direction of the rider in closed loop over time, but has no direct access to the motorcycle's front frame motion or to the rider's brain.

B. Passenger Model

The virtual active passenger's model of the vehicle-rider-passenger system was based on the well-known Acrobot [26]

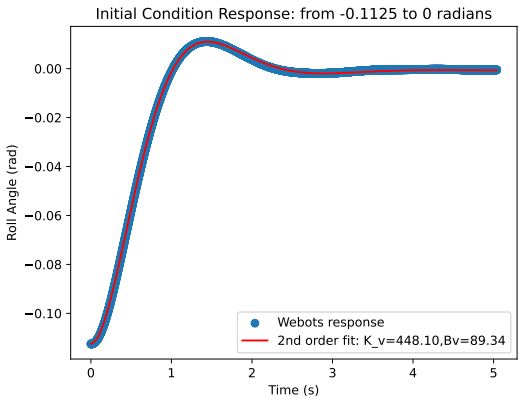

Fig. 1: Initial condition response of the vehicle-rider-rigid passenger system under closed loop steering control in Webots.

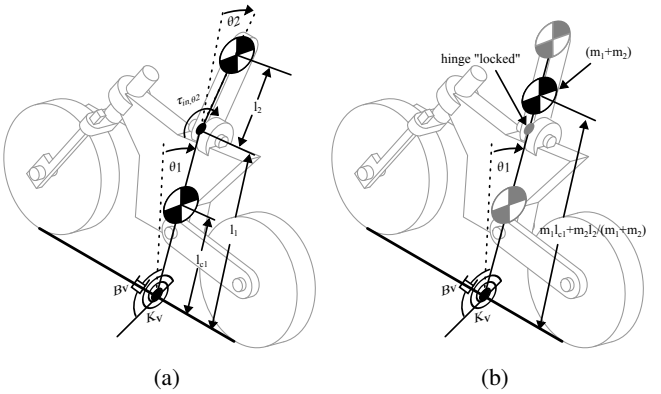

Fig. 2: Model of the rider-vehicle-passenger system with (a) active passenger and (b) rigid passenger

model, which consists of two rigid links pinned together in a hinge-link-hinge-link configuration, with one link pinned to the ground, and a motor actuating the hinge connecting link 1 to link 2. However, we modified the Acrobot model to include a "virtual spring" K_v and a "virtual damper" B_v at the ground hinge to create an approximation of the *rider's* stabilization of the vehicle about the roll axis. The configuration of the modified Acrobot model is shown in Fig. 2a.

Virtual spring and damping constants K_v and B_v were found by fitting a second-order model to the vehicle's closed-loop behavior while the passenger's torso was "locked" in place as if riding while holding on rigidly to the rider. The fit of the closed-loop vehicle-rider-rigid passenger behavior is shown in Fig. 1. The low-order model used to approximate the vehicle's nominal closed-loop behavior as a torsional spring-mass-damper system rotating about the ground contact line, as shown in Fig. 2b, is given in (1).

$$\begin{aligned} T_d = &\left(m_1 l_{c1}^2 + m_2 \left(l_{c1} + l_2\right)^2 + I_1 + I_2\right) \ddot{\theta_1} \\ &+ B_v \dot{\theta_1} + \left(K_v - \left(m_1 + m_2\right)\left(l_1 + l_2\right) g\right) \theta_1 \end{aligned} \tag{1}$$

In (1), T_d is a fictitious disturbance torque, while K_v and B_v represent stabilization efforts by the rider.

With K_v and B_v fit to data from Webots obtained using a rider piloting a vehicle with a rigid passenger (See Fig. 2b), the open-loop model for the active passenger (Fig. 2a) was developed using generalized coordinates $\vec{q} = \begin{bmatrix}\theta_1 & \theta_2\end{bmatrix}^\intercal$. Re-deriving the Acrobot's equations of motion inclusive of K_v and B_v and linearizing about $\theta_1, \theta_2 = 0$ yields a set of two coupled mass-spring-damper equations that can be written in the form of (2). Individual terms in the M, D, and K matrices are given in (3).

$$\begin{aligned} &\underbrace{\begin{bmatrix} M_{11} & M_{12} \\ M_{21} & M_{22} \end{bmatrix}}_{M} \underbrace{\begin{bmatrix} \ddot{\theta}_1 \\ \ddot{\theta}_2 \end{bmatrix}}_{\ddot{q}} + \underbrace{\begin{bmatrix} D_{11} & D_{12} \\ D_{21} & D_{22} \end{bmatrix}}_{D} \underbrace{\begin{bmatrix} \dot{\theta}_1 \\ \dot{\theta}_2 \end{bmatrix}}_{\dot{q}} \\ &+ \underbrace{\begin{bmatrix} K_{11} & K_{12} \\ K_{21} & K_{22} \end{bmatrix}}_{K} \underbrace{\begin{bmatrix} \theta_1 \\ \theta_2 \end{bmatrix}}_{\vec{q}} = \underbrace{\begin{bmatrix} 0 & 0 \\ 0 & 1 \end{bmatrix}}_{F} \underbrace{\begin{bmatrix} \tau_{in,\theta_1} \\ \tau_{in,\theta_2} \end{bmatrix}}_{\vec{u}} \end{aligned} \tag{2}$$

TABLE I: Model Parameters

Symbol	Parameter	Value
l_{c1}	vehicle-rider CoM	0.44 m
l_1	hinge height	0.69 m
l_2	hinge to passenger CoM	0.5 m
m_1	vehicle-rider mass	39.2 kg
m_2	passenger mass	15 kg
I_1	vehicle-rider MOI	7.6 kg-m
I_2	passenger MOI	21.1 kg-m
B_v	rider "virtual damper"	89.3 Nms/rad
K_v	rider "virtual spring"	448.1 Nm/rad

$$\begin{aligned} M_{11} &= m_1 l_{c1}^2 + m_2 l_1^2 + m_2 l_{c2}^2 + 2 m_2 l_1 l_{c2} + I_1 + I_2 \\ M_{12} &= m_1 l_{c2}^2 + 2 m_2 l_1 l_{c2} + I_2 \\ M_{21} &= m_1 l_{c2}^2 + 2 m_2 l_1 l_{c2} + I_2 \\ M_{22} &= m_1 l_{c2}^2 + I_2 \\ D_{12} &= D_{21} = D_{22} = 0 \\ D_{11} &= B_v \\ K_{11} &= K_v - m_1 l_{c1} g - m_2 l_1 g - m_2 l_{c2} g \\ K_{12} &= K_{21} = K_{22} = -m_2 l_{c2} g \end{aligned} \tag{3}$$

In (3), g is the gravitational acceleration constant. τ_{in,θ_1} represents additional input torque exerted about the ground hinge (assumed 0), and τ_{in,θ_2} is the torque exerted by the passenger about the hinge connecting it to the vehicle. Inertias I_1 and I_2 are moments of inertia of the motorcycle-rider system and passenger, respectively, about the mass center of each. Lengths l_{c1} and l_1 refer to the distance from the ground to the mass center of the motorcycle-rider system and the distance from the ground hinge to the passenger hinge, respectively. Length l_2 refers to the distance from the passenger's hinge point to its mass center. Masses m_1 and m_2 refer to the mass of the motorcycle-rider system and passenger, respectively. The parameters used for the virtual passenger's model are shown in Table I.

By rearranging the passenger's model of the vehicle-rider-passenger system given in (2), the model can be written in state space form for use in controller design. Using a state

vector $\vec{x} = \begin{bmatrix}\vec{q} & \dot{\vec{q}}\end{bmatrix}^\intercal$, the state space form of the model can be written as in (4).

$$\underbrace{\frac{d}{dt}\begin{bmatrix}\theta_1\\ \theta_2\\ \dot{\theta}_1\\ \dot{\theta}_2\end{bmatrix}}_{\dot{\vec{x}}} = \underbrace{\begin{bmatrix}0_{2\times2} & I_{2\times2}\\ -M^{-1}K & -M^{-1}D\end{bmatrix}}_{A}\underbrace{\begin{bmatrix}\theta_1\\ \theta_2\\ \dot{\theta}_1\\ \dot{\theta}_2\end{bmatrix}}_{\vec{x}} + \underbrace{\begin{bmatrix}0_{2\times2}\\ M^{-1}F\end{bmatrix}}_{B}\underbrace{\begin{bmatrix}\tau_{in,\theta_1}\\ \tau_{in,\theta_2}\end{bmatrix}}_{\vec{u}} \tag{4}$$

IV. Controller Design

The virtual passenger uses an LQR controller to attempt to stabilize the bike in the upright, "straight running" condition ($[q_1, q_2, \dot{q_1}, \dot{q_2}] = [0, 0, 0, 0]$) using *only* torque τ_{in,θ_2}. To implement a controller that uses τ_{in,θ_2} only, the state space form in (4) was modified to use $B_2 = B\begin{bmatrix}0 & 1\end{bmatrix}^\intercal$ and a single input $u_2 = \tau_{in,\theta_2}$. The LQR controller is based on the state space equation given in (5).

$$\dot{\vec{x}} = A\vec{x} + B_2 u_2 \tag{5}$$

To synthesize the LQR controller, we used the cost function given in (6).

$$J = \int_0^\infty (\vec{x}^\intercal Q\vec{x} + u_2^\intercal R u_2)dt \tag{6}$$

In (6), individual weight matrices are given by (7)

$$Q = \begin{bmatrix}1 & 0 & 0 & 0\\ 0 & 1 & 0 & 0\\ 0 & 0 & 1 & 0\\ 0 & 0 & 0 & 1\end{bmatrix} \tag{7}$$

$$R = \begin{bmatrix}1000\end{bmatrix} \tag{8}$$

The resulting controller, synthesized using the "lqr" function in the Python "control" library, imparts a torque about the passenger-vehicle hinge given by (9).

$$u = -K\vec{x} \tag{9}$$

The weights for the control effort and state error given by (7) were chosen to prioritize low-effort on the part of the passenger while still helping to stabilize the closed-loop vehicle-rider-passenger system.

V. Simulation Setup

To assess the performance of both vehicle-rider-passenger systems (with and without an active passenger) in the face of disturbances from uneven terrain, we used a series of simulations in Webots [5] using the WeBikes add-on [4]. The simulation timestep in all simulations was $1ms$, and tire-ground coulomb friction was set to a coefficient of 1.0. The vehicle model in Webots consisted of a front and rear frame connected by a revolute joint representing the steering axis. The two wheels were connected to the vehicle's front and rear frames using a second revolute joint, along with joints that represent the vehicle's suspension. The passenger was represented as an additional rigid body connected by a revolute joint to the vehicle's rear frame. Parameters of the vehicle and passenger were created to match the parameters in Table I. In each simulation, the vehicle navigated an abrupt change in pavement height, Δh_r, at a speed of 11.2 m/s (roughly 25 mph) while maintaining a goal roll angle of 0°. The test vehicle, experimental setup, and associated nomenclature are summarized in Fig. 3b. We ran simulations of this type for values of Δh_r from 0.125 inches to 3 inches in 0.125-inch increments. Vehicle approach angles α varied from 2° to 20° in 1° increments [4]. For each combination of Δh_r and α, the vehicle was tested with both the rigid passenger and the active passenger.

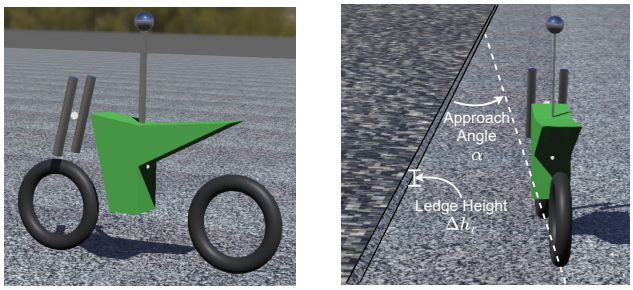

(a) (b)

Fig. 3: Model of motorcycle (a) and annotated test scenario (b) in Webots

The simulation configurations and ranges of α and Δh_r were selected to subject the vehicle to realistic environment-related disturbances that a vehicle might encounter while performing a lane change over uneven pavement, especially on a road that might be under construction. For example, $\alpha > 20°$ are unlikely to be experienced during a normal lane change maneuver at speed. The results of the high-fidelity simulations performed for this range of conditions were intended to shed light on the relative capability of the vehicle equipped with either a rigid passenger or an active passenger in addition to a rider stabilizing the vehicle using steering control. Data collected during each simulation included driver steer torque T_δ, passenger lean angle θ_2, and vehicle roll angle θ_1.

VI. Results

Figure 4 shows the maximum absolute value of vehicle roll angle, $|\theta_1|_{max}$ recorded during each simulation for both the rigid passenger and the active passenger. Figure 5 shows the maximum absolute value of rider steering torque, $|T_\delta|_{max}$ recorded during each simulation for both the rigid passenger and the active passenger. Unsurprisingly, Fig. 4 shows that larger values of $|\theta_1|_{max}$ occur when Δh_r is large (around 3 inches) and when α is at the lower and upper ends of the range simulated. The trend shown in Fig. 5 is similar, with the greatest values of $|T_\delta|_{max}$ occurring in simulations with large Δh_r and with both small and large values of α. While the simulation results show a highly non-linear picture of the vehicle's disturbance rejection performance as α and Δh_r vary, visual inspection of Figs 4 and 5 shows interesting differences between the two controller schemes. The vehicle successfully navigated the step in pavement

height in all simulations, and both controllers were able to maintain the vehicle in an upright configuration with only small changes in vehicle roll angle. This implies that while the passenger never truly "destabilized" the system in its attempts to improve performance, its limited system knowledge does have measurable effects on how the vehicle moves during the maneuver, and how the virtual rider must react.

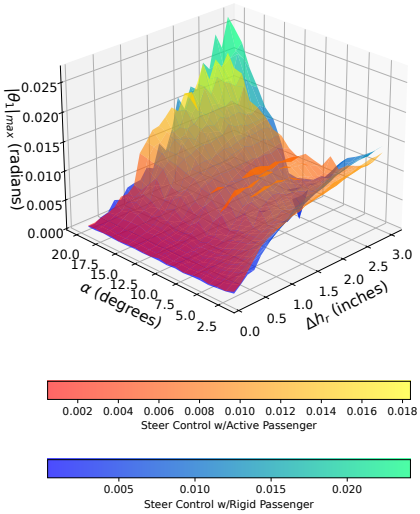

Fig. 4: Maximum roll angle magnitude for vehicle-rider-passenger system with rigid passenger and active passenger during abrupt pavement height transition.

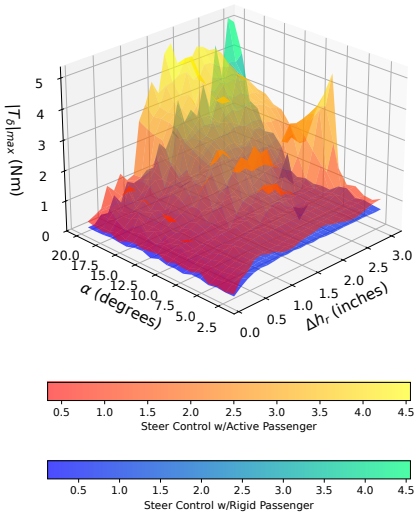

Fig. 5: Maximum rider steer torque magnitude for vehicle-rider-passenger system with rigid passenger and active passenger during abrupt pavement height transition.

If the controller with active passenger represented a unilateral *improvement* over the vehicle with the rigid passenger, we would have expected lower $|\theta_1|_{max}$and $|T_\delta|_{max}$ values from the controller with active passenger. Surprisingly, the two controllers appear to perform differently as the environmental conditions change, indicating that neither approach has a universal advantage. Fig. 6 shows the difference between $|\theta_1|_{max}$ produced by the steering controller with active passenger and $|\theta_1|_{max}$ produced by the steering controller with rigid passenger for each simulation. Fig. 7 shows the difference between $|T_\delta|_{max}$ produced by the steering controller with active passenger and $|T_\delta|_{max}$ produced by the steering controller with rigid passenger for each simulation. Green cells represent positive differences (i.e. that the simulation with active passenger resulted in a larger value than the controller with rigid passenger). Cells that are red therefore represent simulations where the magnitude of either $|T_\delta|_{max}$ or $|\theta_1|_{max}$ was greater with the rigid passenger than with the active passenger. Figures 6 and 7 show that for most small pavement height changes and small approach angles, the difference in max roll angle and max steer torque between the two controller schemes is small. As pavement height changes and approach angle increases, however, more significant differences emerge.

In simulations with the largest Δh_r and α values, $|\theta_1|_{max}$ and $|T_\delta|_{max}$ are significantly smaller with the active passenger, indicating that the active passenger may represent an improvement in overall vehicle disturbance rejection for those simulation conditions.

Conversely, there are also configurations where the rigid passenger has significantly smaller $|\theta_1|_{max}$ and $|T_\delta|_{max}$ values. These configurations appear in an arc shape starting from a 3-inch Δh_r and 9° α and ending at a 1.375-inch Δh_r and 20° α. Over this range of environment configurations, the controller with rigid passenger outperformed the active passenger.

The heterogeneity of the results shown in Figures 6 and 7 could be unique to this vehicle or controller combination, or to the type of disturbance applied. However, they do indicate that a virtual passenger's influence on the overall non-linear vehicle-rider-passenger system behavior is complex *and important*. As researchers work to develop safer infrastructure for motorcycles, and/or advanced safety technologies for motorcycles, it will be critical to include some model of passenger motion in order to get a complete picture of how a new technology or road feature design could affect the dynamics of the vehicle-rider-passenger system.

While Figs. 6 and 7 give an overview of the difference in performance between the two control approaches, understanding how and why the results vary over simulation configurations is difficult when only looking at maximum absolute values of roll angle and steer torque. To examine two cases where the controllers provide the most disparate disturbance rejection, Fig. 8 and Fig. 9 show time-series data from individual tests.

Both time-series data plots demonstrate that when using the steer controller with an active passenger, the bike is more oscillatory leading up to, during, and after traversing the change in pavement height than with a rigid passenger. This behavior is expected, as the active passenger's independent motion makes the vehicle-rider-active passenger system higher order than the rigid passenger system. The active passenger's imperfect model of the vehicle's motion is also a

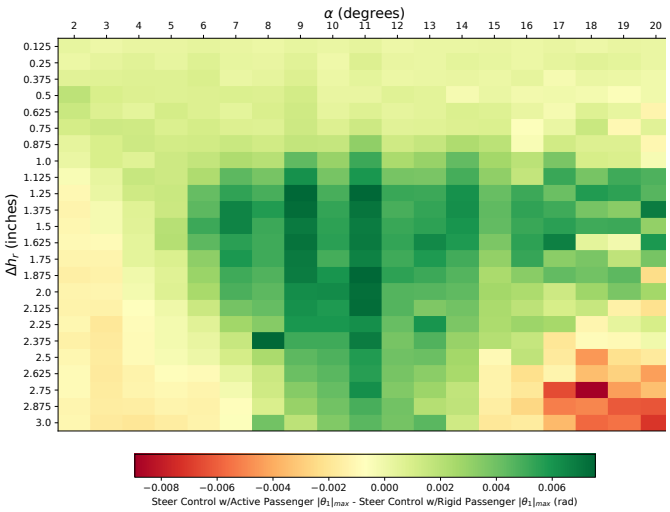

Fig. 6: Heatmap of the difference between the max roll angle recorded for each environment configuration (Steer Control w/Active Passenger - Steer Control w/Rigid Passenger).

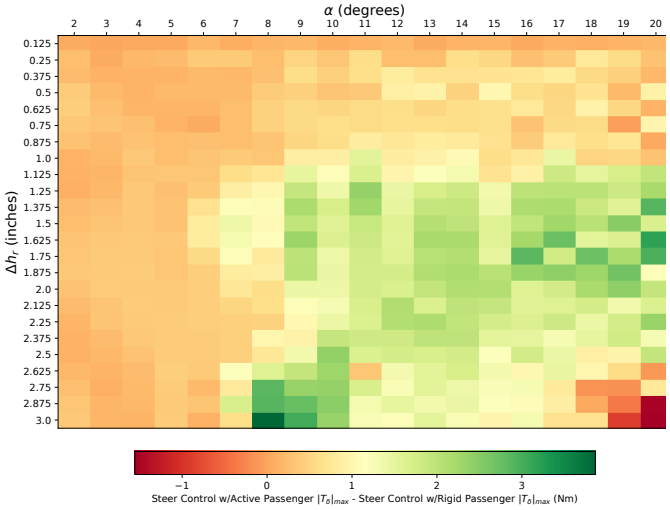

Fig. 7: Heatmap of the difference between the max steer torque recorded for each environment configuration (Steer Control w/Active Passenger - Steer Control w/Rigid Passenger).

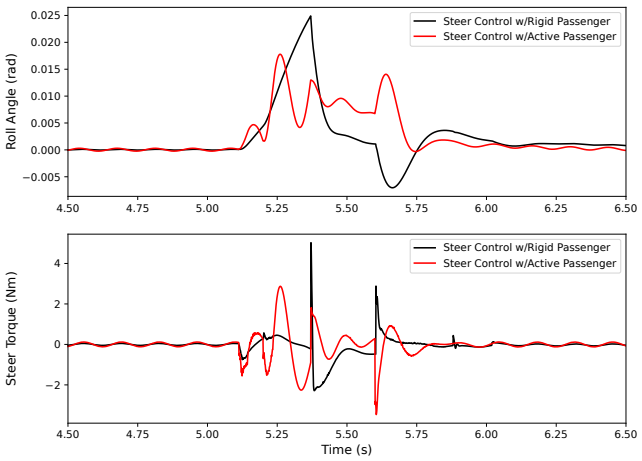

Fig. 8: Time-series plot of vehicle roll angle and rider steer torque with $\Delta h_r = 3$ in, $\alpha = 20°$.

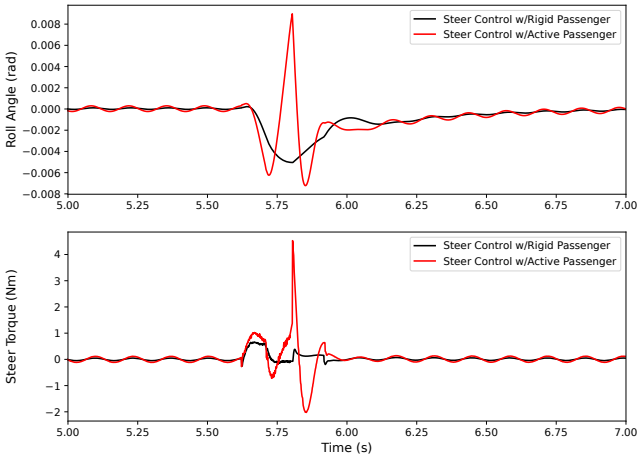

Fig. 9: Time-series plot of vehicle roll angle and rider steer torque for $\Delta h_r = 3$ in, $\alpha = 8°$.

likely contributor to the increase in oscillatory behavior, even though the passenger's control action is *optimal* with respect to its internal model of the vehicle's motion.

As the vehicle traverses the change in pavement height, the active passenger attempts to suppress the deviation in roll angle, with varying levels of success. Fig. 8 shows that when $\Delta h_r = 3$ inches and $\alpha = 20°$, the steer controller with an active passenger was better able to suppress the deviation in roll angle with a smaller maximum steer torque applied. However, when Δh_r is the same but $\alpha = 8°$ (Fig. 9), the active passenger significantly exacerbates the deviation in roll angle which results in a greater maximum steer torque applied by the steer controller in its attempt to maintain vehicle stability.

VII. Conclusion

In this paper, we found that a virtual "active passenger," who has partial, inferred knowledge of the motorcycle's closed-loop roll dynamics but can only influence its motion through torso lean, has mixed effects on a motorcycle's disturbance rejection capability in the face of an uneven pavement feature. At large Δh_r and α values, it was clear that an active passenger improved disturbance rejection and reduced the maximum control input by the rider. However, intermediate values of Δh_r and α resulted showed mixed results, with some configurations favoring the active passenger, and some favoring the passenger who stays still and moves with the vehicle's rear frame.

This study is not without limitations that warrant future investigations on how passenger motion influences both

roadway design and active safety technology design. Human passengers will not behave exactly like either the rigid or active passengers simulated in this study. Motorcycle, rider, passenger, and road parameters vary widely, and the present study only investigates one parameter set and one maneuver. More developed models of both rider and passenger are also possible, and experimental data validating any model of rider or passenger motion is warranted. Extensions to the present work in all of these categories are out of scope for the present paper but are planned as future steps.

However, the results in this study support conclusions from prior work on passenger motion in [2], [3], which indicated that passenger motion can require increased rider effort. We have shown that for a simple road safety simulation study, the relative benefits and disadvantages of passenger motion are complicated. By employing an optimal control strategy for passenger motion, we showed that a passenger acting "in the best interest" of the vehicle-rider-passenger system but with an imperfect model and incomplete state information can either help or hinder *rider* efforts to stabilize and steer the vehicle. This means that as researchers use simulations and/or self-driving surrogate vehicles to develop and evaluate new technology for motorcycle safety, considerations of passenger motion are vital.

REFERENCES

[1] "Motorcycles." [Online]. Available: https://injuryfacts.nsc.org/motor-vehicle/road-users/motorcycles/

[2] T. Koizumi, N. Tsujiuchi, and D. Yasunobe, "Stability Analysis of Tandem Riding on Motorcycles," Nov. 2006, pp. 2006–32–0095. [Online]. Available: https://www.sae.org/content/2006-32-0095/

[3] T. Koizumi, N. Tsujiuchi, Y. Ezaki, and D. Yasunobe, "Analysis of Passenger's Posture Change Effect on Motorcycles and Disturbance Rejection Control," *Journal of System Design and Dynamics*, vol. 2, no. 1, pp. 218–227, 2008.

[4] W. Li, P. Francis, R. McClosky, and A. Brown, "Webikes: a configurable, open-source add-on for simulating single-track vehicle dynamics in the webots robot simulation software," *Advances in Transportation Studies*, vol. Special Vol. 4, pp. 73–88, 2024.

[5] O. Michel, "Webots: Professional mobile robot simulation," *Journal of Advanced Robotics Systems*, vol. 1, no. 1, pp. 39–42, 2004. [Online]. Available: http://www.ars-journal.com/International-Journal-of-Advanced-Robotic-Systems/Volume-1/39-42.pdf

[6] D. J. N. Limebeer and M. Massaro, "The Whipple Bicycle," in *Dynamics and Optimal Control of Road Vehicles*, D. J. N. Limebeer and M. Massaro, Eds. Oxford University Press, Sep. 2018, p. 0. [Online]. Available: https://doi.org/10.1093/oso/9780198825715.003.0005

[7] K. Astrom, R. Klein, and A. Lennartsson, "Bicycle dynamics and control: adapted bicycles for education and research," *IEEE Control Systems Magazine*, vol. 25, no. 4, pp. 26–47, Aug. 2005, conference Name: IEEE Control Systems Magazine. [Online]. Available: https://ieeexplore.ieee.org/document/1499389

[8] M. Araki, K. Akimoto, and T. Takenaka, "Study of Riding Assist Control Enabling Self-Standing in Stationary State," *SAE International Journal of Vehicle Dynamics, Stability, and NVH*, vol. 3, no. 1, pp. 47–56, Dec. 2018. [Online]. Available: https://www.sae.org/content/10-03-01-0004/

[9] D. Bickford and D. E. Davison, "Systematic multi-loop control for autonomous bicycle path following," in *2013 26th IEEE Canadian Conference on Electrical and Computer Engineering (CCECE)*, May 2013, pp. 1–5, iSSN: 0840-7789. [Online]. Available: https://ieeexplore.ieee.org/document/6567714

[10] L. Keo and M. Yamakita, "Control of an Autonomous Electric Bicycle with both Steering and Balancer Controls," *Advanced Robotics*, vol. 25, no. 1-2, pp. 1–22, Jan. 2011. [Online]. Available: https://www.tandfonline.com/doi/full/10.1163/016918610X538462

[11] R. S. Sharp, "On the Stability and Control of the Bicycle," *Applied Mechanics Reviews*, vol. 61, no. 6, p. 060803, Nov. 2008. [Online]. Available: https://asmedigitalcollection.asme.org/appliedmechanicsreviews/article/doi/10.1115/1.2983014/443741/On-the-Stability-and-Control-of-the-Bicycle

[12] D. Limebeer and R. Sharp, "Bicycles, motorcycles, and models," *IEEE Control Systems Magazine*, vol. 26, no. 5, pp. 34–61, Oct. 2006, conference Name: IEEE Control Systems Magazine. [Online]. Available: https://ieeexplore.ieee.org/document/1700044

[13] S. Mammar, S. Espie, and C. Honvo, "Motorcycle modelling and roll motion stabilization by rider leaning and steering torque," in *Proceedings of 2005 IEEE Conference on Control Applications, 2005. CCA 2005.* Toronto, Ont.: IEEE, 2005, pp. 1421–1426. [Online]. Available: https://ieeexplore.ieee.org/document/1507331/

[14] B. Xing, L. Guo, S. Wei, and Y. Song, "Dynamic modeling and robust controller design for circular motion of a front-wheel drive bicycle robot," in *2016 IEEE International Conference on Mechatronics and Automation*, Aug. 2016, pp. 1369–1373, iSSN: 2152-744X. [Online]. Available: https://ieeexplore.ieee.org/document/7558762

[15] Y. Sun, M. Zhao, B. Wang, X. Zheng, and B. Liang, "Polynomial Controller for Bicycle Robot based on Nonlinear Descriptor System," in *IECON 2020 The 46th Annual Conference of the IEEE Industrial Electronics Society*, Oct. 2020, pp. 2792–2797, iSSN: 2577-1647. [Online]. Available: https://ieeexplore.ieee.org/document/9254572

[16] S. Vatanashevanopakorn and M. Parnichkun, "Steering control based balancing of a bicycle robot," in *2011 IEEE International Conference on Robotics and Biomimetics*, Dec. 2011, pp. 2169–2174. [Online]. Available: https://ieeexplore.ieee.org/document/6181613

[17] H. D. Sharma and N. UmaShankar, "A Fuzzy Controller Design for an Autonomous Bicycle System," in *2006 IEEE International Conference on Engineering of Intelligent Systems*, Apr. 2006, pp. 1–6. [Online]. Available: https://ieeexplore.ieee.org/document/1703218

[18] C. Xiong, Z. Huang, W. Gu, Q. Pan, Y. Liu, X. Li, and E. X. Wang, "Static Balancing of Robotic Bicycle through Nonlinear Modeling and Control," in *2018 3rd International Conference on Robotics and Automation Engineering (ICRAE)*, Nov. 2018, pp. 24–28. [Online]. Available: https://ieeexplore.ieee.org/document/8586765

[19] L. Guo, Q. Liao, and S. Wei, "Design of Fuzzy Sliding-mode Controller for Bicycle Robot Nonlinear System," in *2006 IEEE International Conference on Robotics and Biomimetics*, Dec. 2006, pp. 176–180. [Online]. Available: https://ieeexplore.ieee.org/document/4141860

[20] L. Guo, Q. Liao, S. Wei, and Y. Zhuang, "Design of linear quadratic optimal controller for bicycle robot," in *2009 IEEE International Conference on Automation and Logistics*, Aug. 2009, pp. 1968–1972, iSSN: 2161-816X. [Online]. Available: https://ieeexplore.ieee.org/document/5262628

[21] C.-L. Hwang, H.-M. Wu, and C.-L. Shih, "Autonomous dynamic balance of an electrical bicycle using variable structure under-actuated control," in *2008 IEEE/RSJ International Conference on Intelligent Robots and Systems*, Sep. 2008, pp. 3737–3743, iSSN: 2153-0866. [Online]. Available: https://ieeexplore.ieee.org/document/4650588

[22] ——, "A fuzzy decentralized sliding-mode robust adaptive under-actuated control for autonomous dynamic balance of an electrical bicycle," in *2009 IEEE International Conference on Fuzzy Systems*, Aug. 2009, pp. 209–214, iSSN: 1098-7584. [Online]. Available: https://ieeexplore.ieee.org/document/5277246

[23] K. Kanjanawanishkul, "LQR and MPC controller design and comparison for a stationary self-balancing bicycle robot with a reaction wheel," *Kybernetika*, pp. 173–191, Mar. 2015. [Online]. Available: http://www.kybernetika.cz/content/2015/1/173

[24] P. Kondás and P. Kapitány, "Balancing control of a motorcycle," *Pollack Periodica*, Aug. 2022. [Online]. Available: https://akjournals.com/view/journals/606/aop/article-10.1556-606.2022.00612/article-10.1556-606.2022.00612.xml

[25] H. Yetkin, S. Kalouche, M. Vernier, G. Colvin, K. Redmill, and U. Ozguner, "Gyroscopic stabilization of an unmanned bicycle," in *2014 American Control Conference*, Jun. 2014, pp. 4549–4554, iSSN: 2378-5861. [Online]. Available: https://ieeexplore.ieee.org/document/6859392

[26] M. Spong, "The swing up control problem for the Acrobot," *IEEE Control Systems Magazine*, vol. 15, no. 1, pp. 49–55, Feb. 1995, conference Name: IEEE Control Systems Magazine. [Online]. Available: https://ieeexplore.ieee.org/abstract/document/341864